S0021-9797(05)00656-9/FLA AID:11394 Vol.●●●(●●●)
YJCIS:m5 v 1.39 Prn:17/06/2005; 9:51

yjcis11394

[DTD5] P.1 (1-7)
by:violeta p. 1

Available online at www.sciencedirect.com
SCIENCE DIRECT®

ELSEVIER

Journal of Colloid and Interface Science ●●● (●●●●) ●●●–●●●

JOURNAL OF Colloid and Interface Science

www.elsevier.com/locate/jcis

Lead biosorption study with *Rhizopus arrhizus* using a metal-based titration technique

Ghinwa Naja [a], Christian Mustin [b], Jacques Berthelin [b], Bohumil Volesky [a,*]

[a] *Department of Chemical Engineering, McGill University, 3610 University Street, H3A 2B2, Montreal, Quebec, Canada*
[b] *LIMOS, UHP Nancy 1, Faculté des Sciences, Domaine Victor Grignard, B.P. 239, 54506 Vandœuvre les Nancy, France*

Received 22 October 2004; accepted 28 May 2005

Abstract

Acid–base and metal-based potentiometric titration methods were used to analyze sorption mechanisms of lead by *Rhizopus arrhizus* fungal biomass. Biosorption was not considered globally but as the result of successive sorption reactions on various binding sites with different selectivities. Precipitation occurred rapidly when lead concentration increased. Lead was sorbed essentially by carboxylic groups and by phosphates and sulfonates (less abundant) of the organic matter. The lead affinity to carboxylic, sulfonate and phosphate binding sites depended on the association coefficient with proton or counter-ion and on the spatial distribution of the surface sites promoting the formation of mono- or bi-dentate complexes. Chemical bonds and binding sites were confirmed using microscopic and spectroscopic techniques (IR, MET-EDAX). It appeared that although the total organic acidity was reached, number of ionized and free carboxylic groups were not involved in lead sorption reactions. In spite of lead speciation in the solution, surface micro-precipitation was observed and the two processes, surface adsorption and micro-precipitation, are sequential and possibly overlapping. At low concentrations ($<10^{-6}$ M) adsorption is the dominant phenomenon and beyond ($>10^{-5}$ M) surface clusters appeared before the predicted solution precipitation phenomenon.

Keywords: Metal-based high resolution potentiometric titration; Acidic functional groups; Sorption capacity; *Rhizopus arrhizus* fungal biomass

1. Introduction

The influential role of non-living micro-organisms in controlling the mobility and bioavailability of metal ions in aqueous environmental systems is well known and has been extensively studied [1–3]. Biosorption could occur through interactions between metal ions and functional groups of the cell wall biopolymers of dead organisms [4,5].

Chemical mechanisms and ion-binding behavior responsible for biosorption of metal ions by different fungal biomass types remains difficult to describe and model because of their chemical and structural heterogeneity [6]. It has been suggested that specific functional groups are involved in the biomass binding process of heavy metals [7–10].

The present work aimed at studying heterogeneous organic matter (fungus) by quantifying the cell wall functional acidic groups and describing their reactivity. The knowledge of this functional chemical distribution was then employed to explain the most probable mechanism of lead immobilization on the cell wall and to characterize the functional groups of the biomass involved in lead biosorption by *Rhizopus arrhizus* biomass.

The diversity of the functional groups in biomaterials and the polyelectrolytic nature of their organic constituents have suggested that the acid–base and metal-based potentiometric titration methods, previously used to study the formation of soluble organo-metallic complexes [11–13], can help to (1) estimate the total organic acidity of biomaterials, (2) identify the acid ionizable functional groups or binding sites which can play the role of ligands in the presence of protons or lead, and (3) describe the chemical heterogenic reactivity of heterogeneous microbial biomass [14–16].

* Corresponding author. Fax: +1 514 3986678.
E-mail address: boya.volesky@mcgill.ca (B. Volesky).

0021-9797/$ – see front matter © 2005 Published by Elsevier Inc.
doi:10.1016/j.jcis.2005.05.098

S0021-9797(05)00656-9/FLA AID:11394 Vol.●●●(●●●)
YJCIS:m5 v 1.39 Prn:17/06/2005; 9:51
yjcis11394
[DTD5] P.2(1-7)
by:violeta p. 2

The acid–base titration has been developed using proton or hydroxyl as an indicator capable of describing the energy distribution of active sites and defining the optimal capacity of sorption at a certain pH as opposed to general overall capacity. The use of another cation-indicator such as lead, heavier and characterized by a lower diffusion coefficient [17,18], permitted to describe the sorption reaction from another point of view. In order to conduct the lead-titration experiments, an original potentiometric titrator has been developed enabling the analysis of the proton/metal competitions that, in turn, leads to explanation and distinguishing of the mechanisms involved in the lead sorption by fungal biomass. This titrator has various requirements: multi-channel ionometric acquisition (pH and [Pb]), rate, frequency and equilibrium conditions control depending on the chemical reactivity of the heterogeneous solid studied.

2. Materials and methods

2.1. High resolution titrations

All high-resolution titration experiments (acid–base or metal-based) were conducted in a V ml, jacketed glass vessel (Wheaton, 100 or 500 ml, respectively) sealed by a lid fitted with (four or five, respectively) ports for a titrant injection, a N_2 line, a pH electrode and a temperature probe, respectively. An ion selective electrode (lead-ISE) was needed during a metal-based potentiometric titration. The vessel temperature was maintained at 25 °C by recirculation of thermostated water from a bath through the vessel jacket to control the possible temperature effect on the reaction thermodynamics and kinetics. The headspace was purged with N_2 at low pressure during titrations to remove CO_2 and limit its dissolution in the electrolyte and the carbonates formation resulting in the solution pH changes.

2.1.1. Acid–base titrations

Titrant aliquots of a specified volume were injected through a polypropylene line by an automatic and accurate burette (ABU901 Radiometer). The solution in the vessel was agitated by a magnetic stirrer (500 rpm) until pH became stable after each titrant aliquot injection. All experiments were carried out with 0.1 M $NaClO_4$ solution as the background electrolyte. pH was measured using a Ross combined electrode (Ross 8102) and a pH meter (PHM250 Radiometer) after its calibration to IUPAC standards. The inner KCl electrode solution was replaced by a saturated NaCl solution to avoid $KClO_4$ precipitation in the electrode liquid junction. For basic titrations, the titrant used was 0.026 M NaOH solution with a low content of carbonates. Before each biomass titration, a calibration was performed with the background electrolyte previously acidified to pH 2.3 with 0.056 N $HClO_4$, then aliquots of NaOH were added until pH 10.5 is reached.

2.1.2. Metal-based titrations

Titrant aliquots of a specified volume (down to 1 µl ± 0.18%) of 0.001 M $Pb(NO_3)_2$ solution, at pH 5 and of the same ionic strength as the solution in the vessel, were injected through a polypropylene line by an automatic and accurate burette (ABU901 Radiometer) controlled by a microprocessor. The solution in the vessel was agitated by a magnetic stirrer (500 rpm) until pH and E(Pb) became stable after each titrant aliquot injection. All experiments were carried out at pH 5 with 5 mg samples of *R. arrhizus* biomass suspended in 300 ml of $NaNO_3$ as the background electrolyte to maintain an ionic strength of 0.01 M. The selected weight depended on the value of the total organic acidity of the biomass.

pH and E(Pb) were measured using a precise (±0.1 mV) dual-function ionometer (PHM250 Radiometer) linked to (1) a Ross combined electrode (Ross 8102, NaCl saturated) after its calibration with IUPAC standards and to (2) an ion selective electrode (ISE 25 Pb-9, Orion, Radiometer). Directly before each sorbent titration, a calibration was performed with the background electrolyte using the same procedure as for the titrations of solids, to assure the reproducibility of the electrode signal. The maximum acceptable percentage error of the calibration curves slope was 5%. Using an appropriate method, fully discussed in Naja et al. [19], an identical initial electrochemical potential point (−405 ± 5 mV) was obtained, no matter what solid sorbent was examined. The optimized experimental conditions, required to obtain accurate and repeatable results when using a specific ISE, are given in Naja et al. [19]. The accuracy and repeatability of the results after and during the metal-based titrations were verified using the ICP-AES.

The newly developed automated high resolution titration control system permitted to change and specify the operating parameters during titrations such as the volume, rate and frequency of injections, and the stability factor considering the complex nature of each solid to be titrated. The waiting time between any two volume additions was adjusted by the user and depended on the transitional signal (electrochemical potential fluctuations versus time between each two volumes added in order to reach equilibrium) and on the equilibrium condition (dE/dt variations less than 0.2 mV/10 min) by adjusting the number of consecutive constant points with a desired precision. The chosen electrochemical potential stability criterion should take into account the stability of the electrical apparatus and of the electrode signal during the control titration.

The sorbent matter used to study lead biosorption was *Rhizopus arrhizus* fungus (DSM 905) cultivated in a liquid medium [20] at 24 °C in the dark. After 5–6 days of growth, fungal biomass was collected by filtration, ground, washed several times with distilled water to eliminate culture medium residues, lyophilized and stored under vacuum.

2.2. Solution analyses

All chemicals used were of analytical reagent grade. The water used was ultra purified.

After and during the metal-based titration experiments, the solutions were analyzed by (1) ICP-AES (Inductively Coupled Plasma–Atomic Emission Spectrometry, Jobin Yvon JY 238) to verify the lead content detected by the lead selective electrode and by (2) a CHN Analyzer (1106-Carlo Erba) to make sure of the non-existence of amounts of dissolved organic compounds.

The ionic strength of all titration solutions was kept constant and measured by a conductivity meter (CDM 80 Radiometer Conductivity Meter).

2.3. Solid analyses

After lyophilization, organic carbon, hydrogen, nitrogen, phosphorus and sulfur contents in *Rhizopus arrhizus* fungal biomass were determined using a CHN analyzer (1106-Carlo Erba), a TCM DC analyzer (190 Dohrmann) and ICP-AES after an acid digestion (Inductively Coupled Plasma–Atomic Emission Spectrometry, Jobin Yvon JY 238).

The solids after sorption were characterized by Infrared (FTIR) spectrometer and by a High Resolution Scanning Transmission Electron Microscope (Philips CM20/STEM) coupled with an energy dispersive X-ray analyzer (EDXA) used as an elemental analysis tool, capable of identifying the elements in areas less than 0.5 μm in diameter.

To complete the study of the functional groups before and after sorption, an IR analysis was performed with a Fourier Transform Infrared (FTIR) spectrometer (Brüker Vector 22). Each 1 mg dried sample (24 h P_2O_5) was mixed with 200 mg of KBr (Spectranal) and pressed under vacuum. The tablet recovered with a clip, was immediately analyzed with the spectrophotometer in the range of 4000–400 cm^{-1} with a resolution of 1 cm^{-1}. The influence of atmospheric water and CO_2 was always subtracted.

3. Results and discussion

3.1. Rhizopus arrhizus biomass characterizations

The fungal cell wall is characterized by a superposition of chitin layers, proteins and glucans containing important amounts of carboxylic, phosphate, sulfonate and amine groups. *R. arrhizus* biomass preliminary analyses are presented in Table 1 showing organic carbon and nitrogen percentages of 51.9 and 5.04%, respectively, and important quantities of sulfur and phosphorus. Sulfonate groups are involved in the sulfated polysaccharides and some amino acids whereas the phosphonates occur in the phospholipids groups. These moieties are implicated in important chelating groups and should be considered in attempts to explain sorption mechanisms [2,21,22].

Table 1
Amounts of organic carbon, hydrogen, nitrogen, phosphorus and sulfur contained in *Rhizopus arrhizus* (%)

	% C_{org}	% H	% N	% P	% S
Rhizopus arrhizus	51.9	7.8	5.04	1.06	0.83

The organic functional groups and the corresponding wave numbers were identified in the *R. arrhizus* biomass after comparing with other studies addressing infrared spectra of biomass [23,24] or proteins [25,26]. Infrared spectra of *R. arrhizus* biomass (Fig. 1a) showed the presence of amine R–NH_2 (amino acids, proteins, glycoproteins, etc.), carboxylic acids (fatty acids, lipopolysaccharides, etc.), sulfonates and phosphates. The characteristic absorption bands of hydroxyl and amine groups were identified at 3424 and 3276 cm^{-1}, alkyl chains at 2921–2851 cm^{-1}, C=O of the protonated carboxylic groups or esters groups at 1741 cm^{-1}, C=O of the carboxylic groups of aminoacids at 1710 cm^{-1}, C=O of amide groups at 1648 cm^{-1}, COO^- of the carboxylate groups appeared at 1544 and 1418 cm^{-1}, S=O of the sulfonates groups and COO^- groups of the fatty acids were revealed at 1300 cm^{-1}. The wave numbers at 1154–1034 cm^{-1} and 1075 cm^{-1} were attributed to the P–O–C links of the organic phosphated groups and to the P–O of the ($C–PO_3^{2-}$) moiety, respectively. The wave number at 726 cm^{-1} was attributed to the S–O link of the ($C–SO_3^-$) groups.

3.2. Acid–base titration of Rhizopus arrhizus biomass

The potentiometric titration permits quantification of the acid functions eventually involved in lead biosorption. Supposing that a heterogeneous surface exhibits its acidities continuously as a function of the affinity constant (K_a) [27], the titration curves can be adjusted using symmetric Gaussian distribution functions and the total organic acidity (A_{TO}) of a sample could be determined to characterize the organic cell material [28]. The high diffusion coefficient of the proton allowed its access to all the available sites [29] to differentiate the organic functional acidities of the fungal biomass used. Because of the progressive acidic dissociation, three acidity types could be distinguished depending on their apparent ionization constants:

- strong acidities (A_S), attributed to the presence of high affinity acidities such as phosphoric or sulfonate groups as well as carboxylic groups linked to aromatic functions at pH < 4;
- weak acidities (A_W), attributed to the ionization of carboxylic and some proteic groups at 4 < pH < 7; and,
- very weak acidities (A_{VW}), attributed to phenolic and amine groups including the ionization of amino groups of proteins at pH > 7.

Determinations of the acidities and their respective pK_a (Table 2) were carried out using the derivative curves

S0021-9797(05)00656-9/FLA AID:11394 Vol.●●●(●●●)
YJCIS:m5 v 1.39 Prn:17/06/2005; 9:51
yjcis11394
[DTD5] P.4 (1-7)
by:violeta p. 4

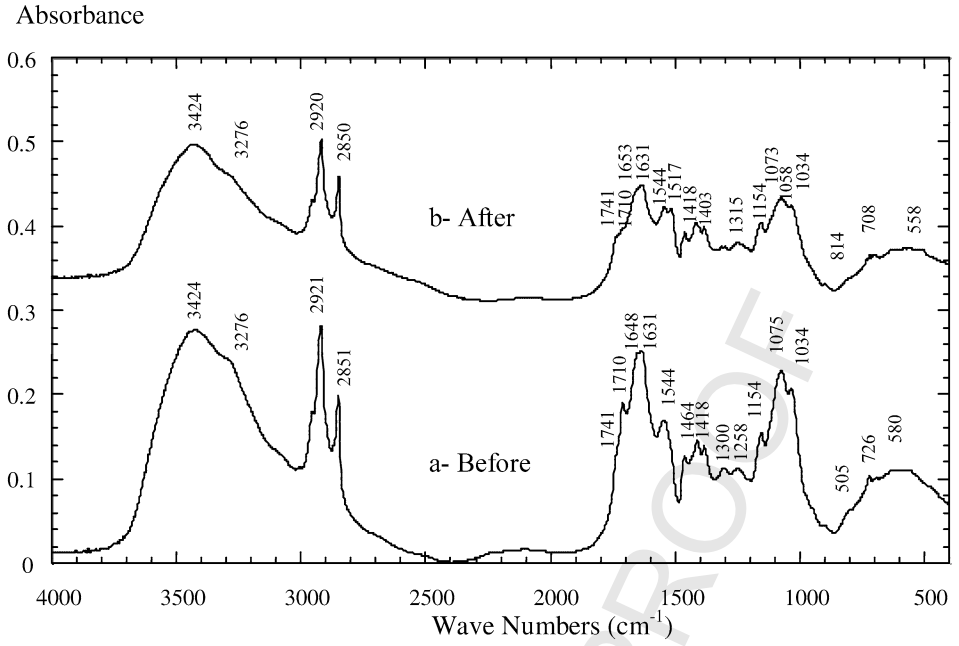

Fig. 1. Infrared spectra of *Rhizopus arrhizus* before (1a) and after (1b) a metal-based potentiometric titration.

Table 2
Types and amounts of acidity (me g^{-1}) and their characteristics (pK_a) for *Rhizopus arrhizus*. A_{TO}, A_S, A_W and A_{VW} represent total organic, strong, weak and very weak acidities, respectively

	A_{TO} (me g^{-1})	A_S (me g^{-1})	A_W		A_{VW}	
			me g^{-1}	pK_{a1}	me g^{-1}	pK_{a2}
Rhizopus arrhizus	2.54	0.27	0.39	4.4	1.88	8.2

$\partial^2 \mathrm{pH}/\partial V^2$, the extrapolation of the Gran's function [30] and the Henderson–Hasselbach representation [31]. The detailed study and the equations used for the quantification of acidities as well as for the determination of their affinity constants are presented in Naja et al. [32]. The method is based on the application of the Gran's equations to a heterogeneous matter where the surface is regarded as a succession and a continuous distribution of acid sites, and the reactions used during an acid–base titration of a multi-polymeric acid are considered. Once the dissociation coefficients α of the acidities were calculated from the progressive acidic dissociation reactions, the Henderson–Hasselbach equation was used to relate the dissociation site coefficients α and the pK_a value to the pH.

R. arrhizus biomass had an A_{TO} of 2.54 me g^{-1} (Table 2), a high value compared to other biomass types. Texier et al. [33] used the same titration technique to study *Pseudomonas aeruginosa* and identified a total organic acidity value of 1.1 me g^{-1}. The high A_{TO} value of the *R. arrhizus* biomass was due to its higher content of amine groups as its cell wall is mainly composed of chitin, linear chains of acetylglucosamine groups, confirmed by a high very weak acidity value $A_{VW} = 1.88$ me g^{-1}.

The strong acidity (A_S) value of 0.27 me g^{-1} for *R. arrhizus* biomass and its weak acidity (A_W) value of 0.39 me g^{-1} confirmed the elemental analysis: the presence of sulfonate, phosphoric and carboxylic moieties. These functional groups could be ionized and thus can possibly participate as active groups in the sorption process [34].

The base titration conducted in the present work showed that while *R. arrhizus* had a total organic acidity of 2.54 me g^{-1} (Table 2), at pH 5 the *R. arrhizus* biomass exhibited only 1.171 me g^{-1} (46%) of the total number of acidic active sites.

Consequently, during a metal uptake experiment, the amount of sorbed metal should be compared to the A_{TO} expressed at a given pH and not to the total organic acidity calculated at the experimental titration final pH value of 10.5.

The acid–base titration provided more information about the functional groups and assisted in defining more precisely the number of active sites at a given pH. The A_{TO} value identified the number of free and available surface sites for a metallic cation and could be considered as an upper accurate limit for the sorption performance.

Combining the Gran and the Hendersson–Hasselbach methods, the pK_a values of the acidities were determined and two major acidity classes were distinguished, the carboxylic, identified by p$K_{a1} = 4.4$, and the amine with a p$K_{a2} = 8.2$. These pK_a values gave a relative idea about the nature of organic groups (inductive effect) linked to carboxylic and amine moieties.

Comparing to the literature [13], the pK_{a1} value obtained in the present work (Table 2) indicated that the carboxylic acidic groups in *R. arrhizus* were linked to aliphatic chains (p$K_a \sim 5.2$ for a carboxylic moiety linked to an aliphatic

chain) rather than to aromatic groups ($pK_a \sim 2.5$ for a carboxylic moiety linked to an aromatic group). The amine ionization constants pK_{a2} of the proteins or polypeptides fall between 8.1 and 9.6 [35], values corresponding to those obtained in the present work.

3.3. Metal-based titration of *Rhizopus arrhizus* biomass

The metal-based potentiometric titration was developed in order to use lead as a second indicator, heavier, having a diffusion coefficient several times lower than protons [17,18] and being more sensitive to the surface site geometry (internal sphere complexes). The metal/proton equilibrium and the synchronism of their exchange effect allowed studying the reactions between the biomass functional groups, lead and protons.

The *R. arrhizus* biomass was demonstrated to possess a high metal sorption uptake (Fig. 2). Indeed, when C_e (equilibrium concentration) $= 1.775$ µmol l^{-1}, lead uptake was about 0.065 mmol g^{-1}. 11% of the binding sites were supposed to be involved in the sorption and the amount of released protons equaled 0.035 mmol g^{-1}. The saturation of the total organic acidity of *R. arrhizus* biomass was observed and could be seen in Fig. 2 as 100% A_{TO}. This saturation occurred at pH 5 for Q_{uptake} $Pb^{2+} = 0.585$ mmol g^{-1}. The values obtained were in accord with values reported in the literature [3] for biomass of other filamentous fungi: 0.589, 0.801 and 0.439 mmol Pb g^{-1} for *Penicillium chrysogenum*, *Rhizopus nigricans* and *Rhizopus arrhizus*, respectively.

The present titration of fungal biomass showed a general progressive decrease of pH (or increase in the quantity of protons released, Fig. 2) and the appearance of several slope changes indicated a different behavior of binding sites.

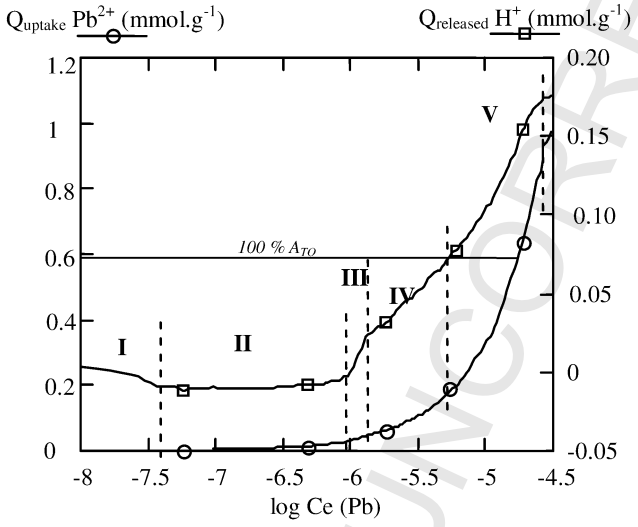

Fig. 2. Lead sorption and proton released mean curves after *Rhizopus arrhizus* metal-based potentiometric titration. I, II, II, IV and V designated the five sorption phases and C_e the equilibrium concentration of lead in solution. More than 100 repeated experimental points were used for the calculations and plotting the figure. The different symbols are used just for differentiating between the two axes.

However, a particular phenomenon was observed at the beginning of the sorption process: an increase of pH was detected followed by a pH stabilization accompanied by a low lead uptake quantity. This phenomenon could be explained by supposing the existence of an important quantity of free binding sites negatively charged in the matrix of the biomass allowing the simultaneous proton and metal sorption. Consequently, there was a competition between the two cations [36]. The proton is small, weakly charged and thus more easily sorbed than lead that occurs as a heavy cation and doubly charged.

Some models that take both ion exchange and Donnan equilibria into account are available in the literature and have been used extensively for the interpretation of polyelectrolyte titration data [37–39]. While the appropriate adaptation of these models for the case of organic matter seems beyond the scope of the present work, the lead sorption and proton-release curves (Fig. 2) could be clearly divided into five phases depending on the co-relation between lead uptake and proton release reflecting the progressive saturation and the reactivity of the sorption sites [40,41]:

- Phase I: the beginning of the sorption process was characterized by a lead non-sorption and by a weak proton sorption. This highly reversible phenomenon is comparable to the Donnan effect observed with resins [42] corresponding to the penetration of charged or not-charged molecules inside pores. It can be explained by the presence of free or sodium binding sites and pores in the fungal biomass matrix. Unlike the lead cation, the proton has a small size and a high intraparticle diffusion coefficient inside the biomass.
- Phase II: during this second phase, pH was quasi-stable and lead was weakly sorbed. This process could be a lead insertion in the fungal biomass matrix or a weak sorption on the sodium sites that did not necessitate the proton release.
- Phase III: this phase was distinguished by an important release of protons in the lead sorption. This process is the real adsorption reaction with establishment of links between the biomass binding carboxylic, polyphosphate or sulfonate sites and lead. An important quantity of protons was being released at the same time and bi-dentate complexes were formed. The latter can be even thermodynamically verified because bi-dentate complexes are more stable than mono-dentates [43].
- Phase IV: this extended phase was characterized by a weak sorption of protons (compared to the third phase) and a more important lead uptake. Sorption was attributed to the formation of mono-dentate complexes between binding sites and lead and to the beginning of the micro-precipitation process on the surface of the biomass [44]. The microscopic observations (Fig. 3) and quantifications (Table 3) confirmed these assumptions.
- Phase V: during this phase, the sorption predicted from the A_{TO} value at pH 5 was exceeded and the sorption up-

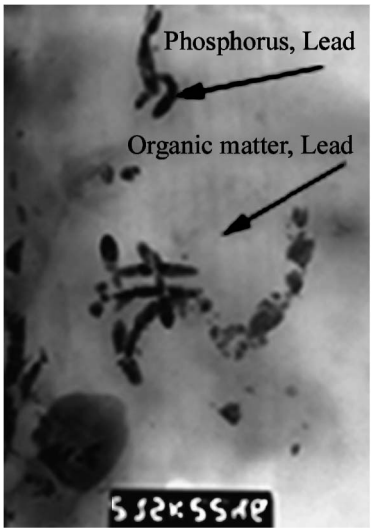

Fig. 3. *Rhizopus arrhizus* photo after lead sorption using a STEM (High Resolution Scanning Transmission Electron Microscope).

Table 3
STEM (EDAX) semi-quantitative results obtained by analyzing *Rhizopus arrhizus* after lead sorption

	% Molar	
	P	Pb
Zone I (lead micro-precipitation)	24.4	59.4
Zone II (rich in organic carbon)	10.6	43.7

take was due in its entirety to a micro-precipitation phenomenon on the surface of the biomass (quasi-vertical slope) [45]. The release of protons was not contradictory and could be explained by the hydroxyl OH^- disappearance during the micro-precipitation of lead as $Pb(OH)_2$ or another hydroxyl-form involving lead. At the end of this process, the two curves (lead uptake and release of protons) formed a plateau indicating the end of the sorption reaction.

To confirm the establishment of binding links between functional groups and lead and the assumption of lead surface micro-precipitation, two techniques were used: Infrared Spectroscopy and a High Resolution Scanning Transmission Electron Microscopy (STEM-EDAX).

The STEM microscope photo (Fig. 3) of the *R. arrhizus* biomass showed that the surface after lead sorption was not homogeneous. Two regions could be highlighted:

The first was identified by organic matter distinguished by the presence of the C, H, N, O elements with lead, and the second characterized by lead micro-precipitation in the presence of phosphorus. This result pointed up the heterogeneity of the sorption process: adsorption on the organic functional groups and lead micro-precipitation in the presence of phosphorus could occur simultaneously. Quantitatively, lead was present in higher quantity in zones rich in phosphorus (Table 3).

The IR spectra of the fungus after lead sorption showed various changes: appearance or disappearance of absorption bands as compared to the fungus spectra before sorption. The corresponding functional groups were identified according to Alberts and Filip [46] and this identification was confirmed when comparisons were made with sodium acetate, lead charged glucose-6-phosphate and lead nitrate spectra. The following observations were noted:

- Unchanged absorption bands at 3276 and 1631 cm^{-1} corresponding to N–H of the amines groups and the C=O of the amides, respectively, indicating that these groups did not participate in lead sorption.
- Decreasing peak intensity at 1710 cm^{-1} corresponding to C=O of the protonated carboxylic acid of the amino acid groups confirming the assumption that the carboxylic groups were involved in the lead sorption. Nevertheless, in spite of the saturation of the total organic acidity at the end of titration, free carboxylic binding groups remained in the biomass that did not complex lead. This phenomenon was probably due first to geometric and steric configuration problems preventing the contribution of all the free carboxylic binding sites predicted as suitable for binding [40,47] and, second, to the micro-precipitation phenomenon blocking the access to free sites [48].
- Splitting of the peaks at 1544 and 1418 cm^{-1} (relative to COO^- groups) and the appearance of new peaks at 1517 and 1403 cm^{-1} characteristic of the COO–Pb associations.
- Decreasing of the intensity of the band intensity at 1154–1034 cm^{-1} and the appearance of a new peak at 1058 cm^{-1} indicating the phosphorus intervention in the lead sorption.
- Slight shifting of peaks from 726 to 708 cm^{-1} indicating the intervention of sulfonates in the lead sorption.

Consequently, using the Infrared Spectroscopy and a High Resolution Scanning Transmission Electron Microscopy (STEM-EDAX), different assumptions could be verified:

- Lead was mainly bound to carboxylic groups of the organic matter and less to its phosphate and sulfonate moieties.
- In spite of the increased lead uptake, higher than the organic total acidity when the saturation of biomass was theoretically reached, number of free carboxylic groups were still not complexed in the fungal biomass.
- Micro-precipitation was promoted at a lead solution concentration less than the total organic acidity and occurred mainly in the presence of phosphate groups. The micro-precipitation phenomenon blocked the access to free sites considered as reactive by the acid–base titration. Micro-precipitation was quickly initialized whenever the solution lead concentration was about 10^{-6} or

10^{-5} M and represented more than 70% of the total sorbed quantity.

– Lead adsorption (*sensu stricto*) occurred at low solution concentrations and contributed modestly to its overall uptake. During the experimental titration, the adsorbed quantity was about 10% of the overall sorbed quantity.

4. Conclusions

The newly developed titrator (acid–base and metal-based) allowed the characterization of the sorption active sites of *Rhizopus arrhizus* biomass and the study of their proton and metal affinity. This experimental approach, combined with infrared spectroscopy, permitted to redefine the biosorption process corresponding, in the majority cases, to the micro-precipitation phenomenon: the real adsorption was associated with weaker concentration ranges. This work redefined the total organic acidity as an upper accurate limit for the sorption performance, offering a higher maximum quantity of free and available surface sites.

A continuum existed between adsorption and precipitation. For a weak site occupation ratio, adsorption was the predominant phenomenon and as the ratio increased, a nucleation occurred, aggregates were formed on the surface and micro-precipitation became the dominant mechanism. Although during titration these processes were sequential, they could occur simultaneously in batches. Because of the structural and chemical heterogeneity of the fungal biomass examined, there was a continuous overlap between sorption process and micro-precipitation phenomenon.

The use of other metals such as cadmium or copper, having different interactions with the biomass structure because of their electrostatic, steric and chemical properties, could complete and confirm the current results.

Acknowledgment

This work was financially supported in part by the Unesco—L'Oréal fellowship for Women in Science.

References

[1] Y. Andres, A.C. Texier, P. Le Cloirec, Environ. Technol. 24 (2003) 1367.
[2] C.L. Brierley, in: H.L. Ehrlich, C.L. Brierley (Eds.), Microbial Mineral Recovery, McGraw-Hill, New York, 1990, p. 303.
[3] B. Volesky, Sorption and Biosorption, BV Sorbex, Montreal, Canada, 2003, p. 316.
[4] R.H. Crist, J.R. Martin, D.R. Crist, Environ. Sci. Technol. 33 (1999) 2252.
[5] J. Marin, J. Ayele, Environ. Technol. 24 (2003) 491.
[6] W.H. Van Riemsdijk, J.C.M. de Wit, L.K. Koopal, G.H. Bolt, J. Colloid Interface Sci. 116 (1987) 511.
[7] D.H. Cho, E.Y. Kim, Bioproc. Biosyst. Eng. 25 (2003) 271.
[8] E. Fourest, C. Canal, J.C. Roux, FEMS Microbiol. Rev. 14 (1994) 325.
[9] G. Sarret, A. Manceau, L. Spadini, J.C. Roux, J.L. Hazemann, Y. Soldo, L. Eybert-Berard, J.J. Menthonnex, Environ. Sci. Technol. 32 (1998) 1648.
[10] Y.Q. Tang, H. Niu, J.H. Wang, B. Volesky, Sichuan Daxue Xuebabo, Gongcheng Kexueban 33 (2001) 50.
[11] G. Brunelot, P. Adrian, J. Rouiller, B. Guillet, F. Andreux, Chemosphere 19 (1989) 1413.
[12] D. Fremstad, 4th Symposium on Ion-Selective Electrodes, Elsevier, Matrafüred, Amsterdam, 1984, p. 383.
[13] S.D. Young, B.W. Bache, D. Welch, H.A. Anderson, J. Soil Sci. 32 (1981) 579.
[14] J. Claessens, T. Behrends, P. Van Cappellen, Aquat. Sci. 66 (2004) 19.
[15] S.B. Pandeya, A.K. Singh, Plant Soil 223 (2000) 13.
[16] C. Rey-Castro, P. Lodeiro, R. Herrero, M.E.S. De Vicente, Environ. Sci. Technol. 37 (2003) 5159.
[17] D. Dobos, A Handbook for Electrochemists in Industry and Universities, Elsevier Scientific, Amsterdam, 1994, p. 88.
[18] A.L. Horvath, A Handbook of Aqueous Electrolyte Solutions, Ellis Horwood, West Sussex, UK, 1985, p. 289.
[19] G. Naja, C. Mustin, B. Volesky, J. Berthelin, Chemosphere, in press.
[20] J.C. Roux, B. Lhomme, B. De Vôgue, J. Neyton, J.P. Teisador, Société Française de Microbiologie (1988) 233.
[21] R.H. Crist, K. Oberholser, N. Shank, M. Nguyen, Environ. Sci. Technol. 15 (1981) 1212.
[22] S. Markai, Y. Andres, G. Montavon, B. Grambow, J. Colloid Interface Sci. 262 (2003) 351.
[23] J.R. Heber, R. Stevenson, O. Boldman, Science 116 (1952) 111.
[24] J. Schmitt, H.C. Flemming, Int. Biodeterior. Biodegrad. Sci. 41 (1998) 1.
[25] R.M. Gendreau, R.I. Leininger, S. Winters, R. Jacobsen, Biomaterials 1 (1982) 371.
[26] R.M. Silverstein, G.C. Bassler, Spectrometric Identification of Organic Compounds, Wiley, New York, 1964, p. 177.
[27] J.C.M. de Wit, W.H. Van Riemsdijk, L.K. Koopal, Environ. Sci. Technol. 27 (1993) 2005.
[28] G. Sposito, K.M. Holtzclaw, Soil Sci. Soc. Am. J. 3 (1977) 330.
[29] J. Yang, B. Volesky, Environ. Sci. Technol. 33 (1999) 751.
[30] G. Gran, Analyst 77 (1952) 661.
[31] F.J.C. Rossotti, H. Rossotti, J. Chem. Educ. 42 (1965) 375.
[32] G. Naja, C. Mustin, B. Volesky, J. Berthelin, Water Res. 39 (2005) 579.
[33] A.C. Texier, Y. Andres, M. Illemassene, P. Le Cloirec, Environ. Sci. Technol. 34 (2000) 610.
[34] B. Greene, R. McPherson, D. Darnall, in: J.W. Patterson, R. Pasino (Eds.), Metals Speciation, Separation and Recovery, Lewis, Chelsea, MI, 1987, p. 315.
[35] A.E. Martell, R.D. Hancock, R.J. Motekaitis, Coord. Chem. Rev. 133 (1994) 39.
[36] C. Huang, C.P. Huang, A.L. Morehart, Water Res. 25 (1991) 1365.
[37] J.A. Marinsky, J. Ephraim, Environ. Sci. Technol. 20 (1986) 349.
[38] C. Rey-Castro, P. Lodeiro, R. Herrero, M.E.S. de Vicente, Environ. Sci. Technol. 37 (2003) 5159.
[39] S. Schiewer, B. Volesky, Environ. Sci. Technol. 30 (1996) 2921.
[40] A.M. Scheidegger, D.L. Sparks, Soil Sci. 161 (1996) 813.
[41] D.L. Sparks, Environmental Soil Chemistry, Academic Press, San Diego, SA, 1995, p. 2746.
[42] M. Pesavento, R. Biesuz, React. Funct. Polym. 36 (1998) 135.
[43] W. Stumm, Chemistry of the Solid–Water Interface, Wiley, New York, 1992, p. 448.
[44] L.E. Macaskie, A.C.R. Dean, A.K. Cheetham, R.J.B. Jakeman, A.J. Skarnulis, J. Gen. Microbiol. 133 (1987) 539.
[45] I.T. Mayers, T.J. Beveridge, Can. J. Microbiol. 35 (1989) 764.
[46] J.J. Alberts, Z. Filip, Environ. Technol. 19 (1998) 923.
[47] G. Naja, Ph.D. Thesis, Henri-Poincaré University, Nancy, France, 2001, p. 255.
[48] D.A. Dzombak, F.M.M. Morel, Surface Complexation Modeling. Hydrous Ferric Oxide, Wiley, New York, 1990, p. 391.